ANALYTICAL SCIENCES AUGUST 2018, VOL. 34

Phase Separation Multi-phase Flow Using an Aqueous Two-phase System of a Polyethylene Glycol/Dextran Mixed Solution

Naoya IMANISHI,* Tetsuo YAMASAKI,* Kazuhiko TSUKAGOSHI,*,† and Masaharu MURATA*****

**Department of Chemical Engineering and Materials Science, Faculty of Science and Engineering, Doshisha University, Kyotanabe, Kyoto 610–0321, Japan*
***Bio-Microfluidic Science Research Center, Doshisha University, Kyotanabe, Kyoto 610–0321, Japan*
****Innovation Center for Medical Redox Navigation, Kyushu University, 3-1-1 Maidashi, Higashi, Fukuoka 812–8582, Japan*

Polyethylene glycol/dextran mixed solution as an aqueous two-phase system was fed into a fused-silica capillary tube under different conditions, resulting in phase transformation leading to phase separation multi-phase flow through/along a liquid–liquid interface. As one flow-type example, when 6.4 wt% polyethylene glycol and 9.7 wt% dextran aqueous solution containing 1.0 mM Rhodamine B was fed into the capillary tube at 3°C, tube radial distribution flow (annual flow) was observed through bright-field microscopy. Tube radial distribution flow consisted of a dextran-rich inner phase and polyethylene glycol-rich outer phase. We also examined the distribution of proteins, such as bovine serum albumin, hemoglobin, and lysozyme, in the inner and outer phases through use of double capillary tubes with different inner diameters. The protein distribution was greater in the inner (dextran-rich) phase than the outer (polyethylene glycol-rich) phase. The distribution ratios of the three proteins (ratio of the inner/outer protein concentration) were 2.3, 4.2, and 1.8, respectively. The proteins concentrated in the dextran-rich phase through tube radial distribution flow of a polyethylene glycol/dextran mixed solution.

Keywords Phase separation multi-phase flow, polyethylene glycol, dextran, aqueous two-phase system, tube radial distribution flow

(Received March 9, 2018; Accepted April 17, 2018; Published August 10, 2018)

Introduction

Aqueous two-phase systems (ATPS) are formed when either two polymers, one polymer and one kosmotropic salt, or two salts (one chaotropic salt and one kosmotropic salt) are mixed at appropriate concentrations or at particular temperatures. They have been used for many years in biotechnological applications as non-denaturing and benign separation media.[1-4] Recently, Hamta *et al*. found that ATPS can be used for the separation of metal ions like mercury and cobalt.[5]

Subsequent investigation led to the determination of many other aqueous biphasic systems, of which the polyethylene glycol (PEG)/dextran system is the most extensively studied. The "upper phase" is formed by the more hydrophobic PEG, and has lower density than the "lower phase," consisting of the hydrophilic and denser dextran solution. Based on this two-phase system, liquid–liquid and liquid–solid extractions have been reported using various types of PEG/dextran mixed solution.[6-8]

We recently developed a method to generate a multi-phase flow using two-phase separation mixed solvent solutions, such as water–hydrophilic–hydrophobic organic ternary mixed solvent solutions,[9] ionic liquid–water mixed solutions,[10] fluorocarbon–hydrocarbon organic mixed solvent solutions,[11] *etc.* The two-phase separation mixed solvent solutions undergo phase transformation under changing temperature and/or pressure, leading to upper and lower phases in batch vessels. On the other hand, when the mixed solvent solutions are delivered into a microspace, such as a microchannel on a microchip or a capillary tube, phase transformation also occurs in the microfluidic flow, generating kinetic liquid–liquid interfaces.[12-16]

These new types of multi-phase flows are referred to as "phase separation multi-phase flows," and are distinguished from conventional immiscible multi-phase flows. Of particular interest is their ability to generate annular flows, with inner and outer phases. The specific microfluidic phenomenon and flow are referred to as the "tube radial distribution phenomenon" (TRDP) and "tube radial distribution flow" (TRDF), respectively.[12-16] Relevant considerations and data have been reviewed in our previous studies.[17,18] For example, when water–hydrophilic–hydrophobic organic solvent mixtures are delivered into a microspace, the solvent molecules radially distribute, generating inner and outer phases. TRDF creates a phase interface or kinetic liquid–liquid interface within the microspace. TRDF has been applied to new types of chromatography, extraction, mixing, and microreactor systems.

However, the data from these experiments are assumed to be only the first in a new field of TRDP and related research, as TRDP involves a rather novel microfluidic behavior yet to be fully investigated. It is important to continue examining the

† To whom correspondence should be addressed.
E-mail: ktsukago@mail.doshisha.ac.jp

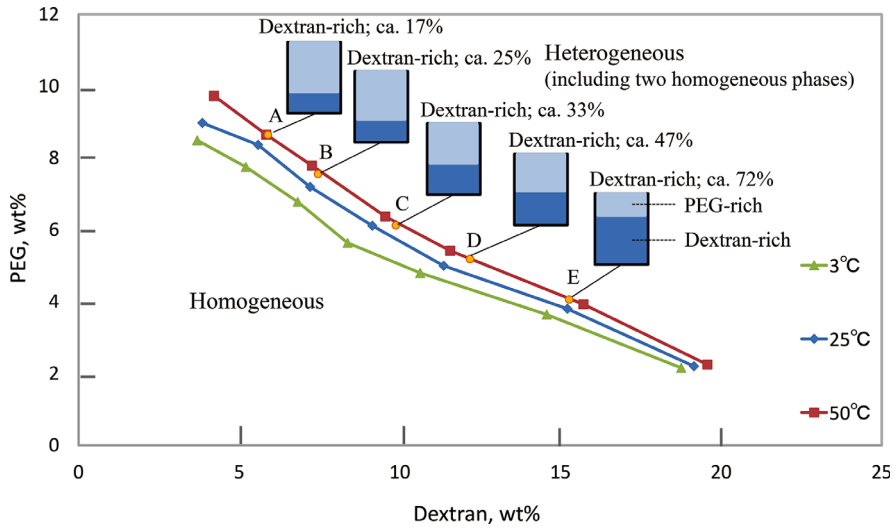

Fig. 1 Phase diagrams of PEG/dextran mixed solutions at 3, 25, and 50°C. The three lines indicate solubility curves; the area below the lines is homogeneous and area above is heterogeneous including the two phases. The components of mixed solutions A, B, C, D, and E are: A (PEG 8.3 wt% and dextran 5.6 wt%), B (PEG 7.5 wt% and dextran 7.5 wt%), C (PEG 6.4 wt% and dextran 9.7 wt%), D (PEG 5.1 wt% and dextran 12.1 wt%), and E (PEG 3.8 wt% and dextran 15.1 wt%). When the solutions A – E are cooled from 50 to 3°C, they change from homogeneous to heterogeneous including upper (PEG-rich solution) and lower (dextran-rich solution) phases as shown in the figure.

fundamental properties of TRDP as much as possible. In this first-time performed study, a PEG/dextran mixed solution formed from polymer-dissolved aqueous solution as one of the ATPS as opposed to solvent mixed solution, which displayed two-phase separation in a batch vessel, was fed into a capillary tube to explore TRDP. TRDP or TRDF based on the ATPS without using any organic solvents is attractive for biomolecule analysis and science. We report as a result the importance of understanding TRDF capacity, and related technological applications.

Experimental

Reagents and materials

Water was purified using an Elix 3 UV (Millipore Co., Billerica, MA). All reagents were commercially available and of analytical grade. PEG, dextran, Rhodamine B, bovine serum albumin (BSA), and lysozyme were purchased from Wako Pure Chemical Industries, Ltd. (Osaka, Japan). Hemoglobin was purchased from Nacalai Tesque (Kyoto, Japan). Fused-silica capillary tubes (50, 75, 100, and 200 μm inner diameter) were purchased from GL Sciences (Tokyo, Japan).

Viscosity measurement

The homogeneous solutions of all mixed solvent systems were converted in batch vessels to heterogeneous solution systems that comprised two phases—upper and lower—by controlling the temperature. The viscosities of the mixture solutions as well as the upper and lower solutions were measured with a viscometer (HAAKE RheoScope 1; Thermo Scientific, Sydney, Australia).

Bright-field microscope-charged-couple device (CCD) camera system

The bright-field microscope-CCD camera system was equipped with a fused-silica capillary tube. The ternary mixed solvent solution with and without Rhodamine B introduced into the capillary tube was observed using a microscope (BX51; Olympus, Tokyo, Japan) and a CCD camera (JK-TU53H; Toshiba, Tokyo, Japan) for bright-field imaging. The addition of Rhodamine B made it easy to observe multi-phase flows except an annular flow. The temperature of the capillary tube was controlled using a thermo-heater (Thermo Plate MATS-555RO; Tokai Hit Co., Shizuoka, Japan).

Results and Discussion

Phase diagram of PEG/dextran mixed solution

The phase diagram of PEG/dextran mixed solution was examined at temperatures of 3, 25, and 50°C (Fig. 1). The solubility curves in the diagram indicate the boundary between the homogeneous and heterogeneous solutions including the two phases. The components of PEG/dextran mixed solutions of A – E are noted in the caption of Fig. 1. After the homogeneous mixed solutions of A – E were cooled from 50 to 3°C, the homogeneous solution turned heterogeneous with upper (PEG-rich solution) and lower (dextran-rich solution) phases. The volume ratios of the heterogeneous solutions were estimated through visual observation in a glass vessel. They are also shown in Fig. 1 as a volume percentage of dextran-rich phase.

Tube radial distribution flow

The homogeneous PEG/dextran mixed solutions (A – E in Fig. 1) prepared at 50°C remained homogeneous as they had been kept at 25°C for at least 6 h. Homogeneous mixed solutions (A – E) containing Rhodamine B were fed into the capillary tube at 25 and 3°C for visualization. The observed bright-field microscope photographs are shown in Fig. 2 and conditions are described in the caption. The homogeneous flows were observed for all solutions at 25°C, while the heterogeneous flows having liquid–liquid interface, that is, phase

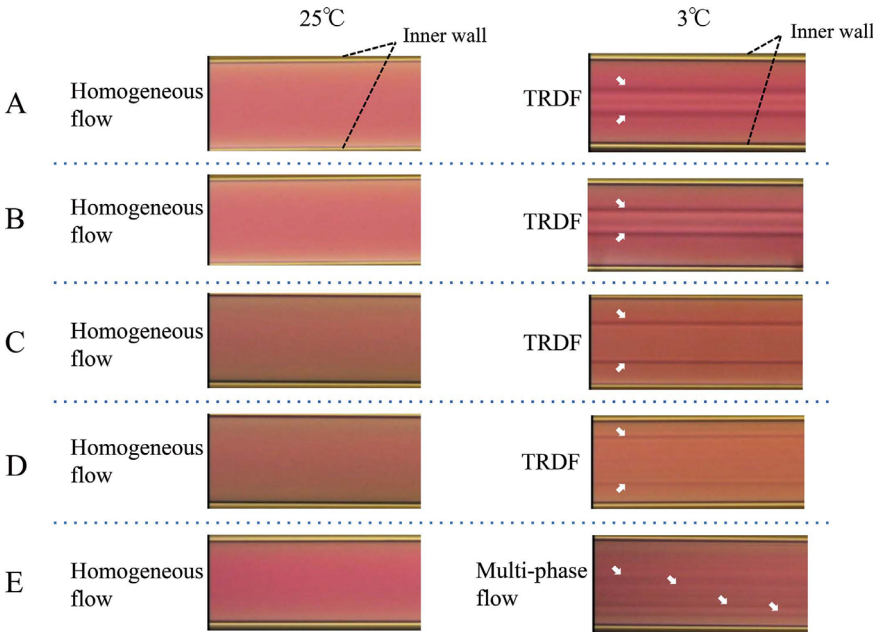

Fig. 2 Bright-field photographs observed for PEG/dextran mixed solutions in the capillary tube. Fused-silica capillary, 50 μm i.d., 120 cm (observation point, 20 cm from the capillary outlet and cooling length, *ca.* 80 cm); temperature, 3 and 25°C; flow rate, 0.1 μL min^{-1}. Components of PEG/dextran mixed solutions A – E are described in Fig. 1 containing 1.0 mM Rhodamine B.

Table 1 The microfluidic behavior for solutions C and D at various flow rates and temperature

Temp.	Solution C				Solution D			
	0.1 – 0.5 μL min^{-1}	0.8 – 2.0 μL min^{-1}	3.0 – 8.0 μL min^{-1}	10.0 – 20.0 μL min^{-1}	0.1 – 0.5 μL min^{-1}	0.8 – 2.0 μL min^{-1}	3.0 – 8.0 μL min^{-1}	10.0 – 20.0 μL min^{-1}
3°C	TRDF	TRDF	TRDF	Multi-phase flow	TRDF	TRDF	Multi-phase flow	Multi-phase flow
15°C	TRDF	Multi-phase flow	Multi-phase flow	Homogeneous	Multi-phase flow	Multi-phase flow	Homogeneous	Homogeneous
25°C	Multi-phase flow	Homogeneous	Homogeneous	Homogeneous	Homogeneous	Homogeneous	Homogeneous	Homogeneous

Fused-silica capillary, 50 μm i.d., 120 cm (observation point, 20 cm from the capillary outlet and cooling length, *ca.* 80 cm), and PEG/dextran mixed solution C (PEG 6.4 wt% and dextran 9.7 wt%) and D (PEG 5.1 wt% and dextran 12.1 wt%) containing 1.0 mM Rhodamine B.

separation multi-phase flow, were observed at 3°C based on phase transformation. TRDF was observed for solutions A – D and multi-phase flow was observed for solution E. The multi-phase flow generated through phase separation but did not perform annular flow or TRDF. They were also confirmed at about several cm from the cooling without large difference between solutions A – D. The flow conditions required for TRDF and multi-phase flow could be considered by examining dimensionless numbers including inertial force, interfacial tension, and viscous force as basic fluidic factors in the next step.[14] As shown in Fig. 1, dextran-rich phase volumes increased from *ca.* 17 to 47% from solution A to D. Also, in Fig. 2, the inner phase volumes in TRDF gradually increased from solution A to D. The inner and outer phases in TRDF were dextran-rich and PEG-rich solutions, respectively, determined from their volume ratios.

Effects of flow rates and temperature were also examined for the mixed solutions C and D on phase separation multi-phase flow. Table 1 summarizes the microfluidic behavior for solutions C and D at various flow rates and temperature. The lower flow rate (0.1 – 0.5 μL min^{-1}) and the lower temperature (3°C) generated stable TRDF. The homogeneous flows were generally observed at 25°C. TRDF was observed in the capillary having 75, 100, and 200 μm inner diameter (the data not shown).

Separation of proteins using microflow system with different inner diameter double tubes

A schematic diagram of the microflow separation system using double capillary tubes[19] with different inner diameters (75, 100, and 200 μm) is shown in Fig. 3(a). The PEG/dextran mixed solution, C (PEG 6.4 wt% and dextran 9.7 wt%), was delivered into the large capillary and resulting TRDF observed as per Fig. 3(b). The inner (dextran-rich) and outer (PEG-rich) phases were separated into the inside-smaller tube (75 μm i.d. and 150 μm o.d.) and outside-smaller tube, respectively, not including any absorption operation from capillary tube outlets. The specific flow of the inner phase in capillary A into capillary B inside was performed under the present conditions described in Fig. 3, that were experimentally determined, mainly by changing the length of capillary C.

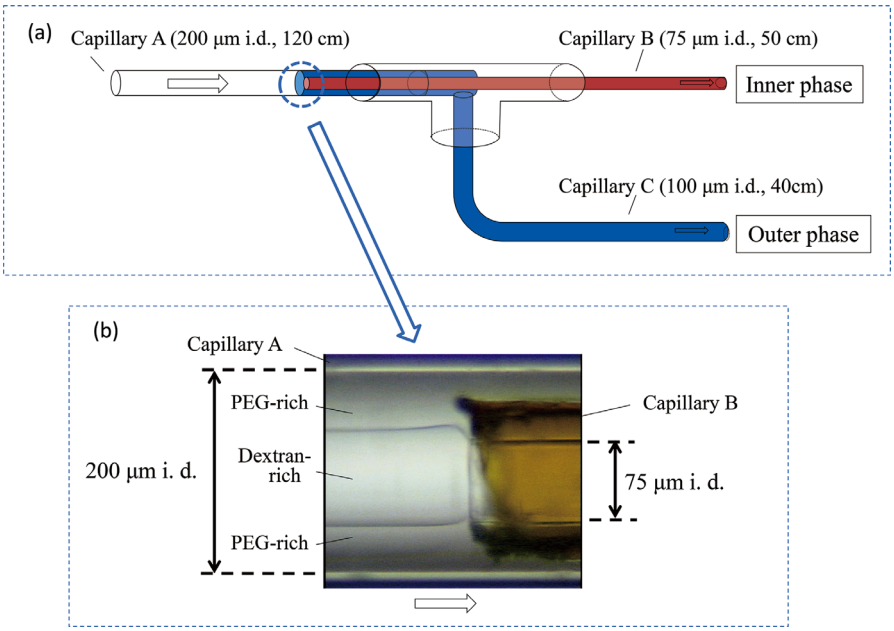

Fig. 3 Microflow separation system. (a) Schematic diagram of the system using double capillary tubes with different inner diameters, and (b) the bright-field microscope photograph at the inlet of the smaller capillary. The inner diameters of fused-silica capillary A, B, and C are described in the figure. Temperature, 3°C; flow rate, 50 μL min^{-1}; PEG/dextran mixed solution C (PEG 6.4 wt% and dextran 9.7 wt%).

The distribution of proteins, such as BSA, hemoglobin, and lysozyme, between the lower (dextran-rich) and upper (PEG-rich) phases obtained through phase transformation of the homogeneous solution was first examined for the PEG/dextran mixed solution C in the batch vessel, where water was exchanged with 200 mM of phosphate buffer of pH 7.0. The PEG/dextran mixed solution (8 mL) containing 1.5 g L^{-1} protein was cooled from 25 to 3°C and separated to the upper and lower phases, which took *ca.* 30 min. After separation, the protein concentration in the upper and lower phases was examined by absorption spectrophotometry calibration method (280 nm for BSA and lysozyme; 400 nm for hemoglobin). The distribution ratios (ratios of the lower/upper protein concentrations) of BSA, hemoglobin, and lysozyme in the batch vessel were 2.8, 4.4, and 1.9, respectively.

Similarly, protein distribution was examined between the inner (dextran-rich) and the outer (PEG-rich) phases in TRDF using the microflow separation system. The PEG/dextran mixed solution C containing 1.5 g L^{-1} protein was fed at a flow rate of 50 μL min^{-1}, cooling from 25 to 3°C to produce TRDF. The inner (dextran-rich) and outer (PEG-rich) phases were respectively recovered through capillaries B and C. Protein was also continuously recovered from B and C through TRDF using the separation system, concentrating in the inner (dextran-rich) phase. After separation, protein concentration in the inner and outer phases was examined by absorption spectrophotometry calibration method (280 nm for BSA and lysozyme; 400 nm for hemoglobin). The distribution ratios of BSA, hemoglobin, and lysozyme in TRDF were 2.3, 4.2, and 1.8, respectively. Protein distribution is thought to be, first, performed through heterogeneity of protein concentration in the process of phase separation, and subsequently, reach equilibrium in the TRDF in capillary A, having the constant length of 120 cm. Nearly the same ratios of the three proteins were obtained using the batch vessel and TRDF microflow separation system.

Separation of co-existing hemoglobin and lysozyme using microflow system

Distributions of co-existing hemoglobin and lysozyme were examined between the inner (dextran-rich) and the outer (PEG-rich) phases in TRDF obtained with the microflow separation system. Hemoglobin and lysozyme showed the most varied distribution ratios among the three proteins. The PEG/dextran mixed solution C containing 1.5 g L^{-1} of each protein was fed at a flow rate of 50 μL min^{-1}, cooling from 25 to 3°C to give TRDF. The inner (dextran-rich) and outer (PEG-rich) phases were respectively recovered through capillary B and C. Proteins were continuously recovered into B and C through TRDF using the separation system, concentrating in the inner (dextran-rich) phase. After separation, protein concentrations in the inner and outer phases were examined by absorption spectrophotometry calibration method (280 and 400 nm for hemoglobin and 280 nm for lysozyme). The distribution ratios of hemoglobin and lysozyme (the ratios of the inner/outer protein concentrations) in TRDF were 4.1 and 1.9, respectively. Similar distribution ratios of the two proteins were obtained with individual and coexisting proteins in TRDF separation.

As hemoglobin and lysozyme had different distribution ratios, the solution collected from the inner phase contained a higher concentration of hemoglobin compared to the original mixed solution; hemoglobin and lysozyme concentrations were both 1.5 g L^{-1} in the original solution, 2.5 and 1.9 g L^{-1} in the collected solution from the inner phase, and 0.61 and 1.0 g L^{-1} in the collected solution from the outer phase, respectively. The results demonstrated that the present microflow system was useful for the separation and extraction of biomolecules such as proteins. The present system can deal with a small amount of solutions and in a short time in a microspace, similarly to microchip devices, compared to common batch systems. Also, the separation and extraction in the system is performed in a one-flow line system, leading to simplification.

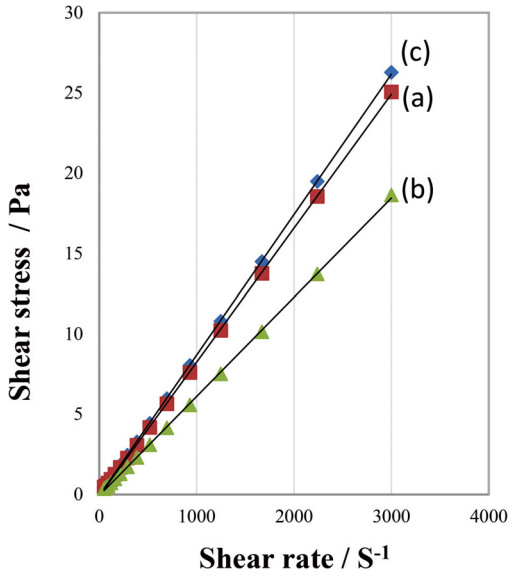

Fig. 4 Relationships between share rate and share stress in PEG/dextran mixed solution C (PEG 6.4 wt% and dextran 9.7 wt%) for (a) the mixture solution, (b) the upper (PEG-rich), and (c) lower (dextran-rich) solutions in a batch vessel separated through phase transformation by cooling.

Considerations based on viscous dissipation[15]

The PEG/dextran mixed solution C (PEG 6.4 wt% and dextran 9.7 wt%) was separated into upper (PEG-rich) and lower (dextran-rich) solutions through phase transformation by cooling. The viscosities of mixed, upper, and lower solutions were 0.0082, 0.0059, and 0.0086 [Pa·s], respectively; they were relatively large compared to water and organic solvent such as acetonitrile and ethyl acetate. Figure 4 shows the relationship between shear rate and shear stress for the three solutions. The good linearity verifies their behavior as Newtonian fluids. In order to theoretically confirm the phase configuration of the inner (dextran-rich) and outer (PEG-rich) solutions in TRDF, we calculated viscous dissipation energies based on Newtonian fluids.

In fluid mechanics, viscous dissipation is manifested by the transformation of kinetic energy into thermal energy through fluidic viscosity. According to the principle of viscous dissipation, fluidic flow maintains the solvent distribution determined by the minimum value extracted from the equation. Here, the phase configuration in TRDF was considered from viscous dissipation principles, incorporating the separation system with double tubes (or TRDF in the capillary of 200 μm inner diameter) as an example.

To derive concrete equations of viscous dissipation, typical annular flows in an immiscible multi-phase flow were examined. One shows the solvent distribution featuring the higher viscosity solvent as the inner phase (Case 1) and another shows the solvent distribution featuring the lower viscosity solvent as the inner phase (Case 2).

The total viscous dissipation energy (E_t) can be calculated by combining the energies for the inner (E_i) and outer phases (E_o), *i.e.* $E_t = E_i + E_o$.

According to the previous paper,[15] E_t for the Case 1 is expressed as follows, where Q_t is the total flow rate, r_{int} and r_{wall} are the distances from the center of the tube to the liquid–liquid interface and to the inner wall, respectively, μ_1 and μ_2 are viscosities ($\mu_1 < \mu_2$).

$$E_t = E_i + E_o = \frac{4{Q_t}^2}{\pi\left(\frac{r_{wall}^4 - r_{int}^4}{\mu_1} + \frac{r_{int}^4}{\mu_2}\right)}$$

In addition, E_t for Case 2 is:

$$E_t = E_i + E_o = \frac{4{Q_t}^2}{\pi\left(\frac{r_{int}^4}{\mu_1} + \frac{r_{wall}^4 - r_{int}^4}{\mu_2}\right)}$$

Values of $Q_t = 8.33 \times 10^{-10}$ m^3 s^{-1}, $\mu_1 = 0.0059$ Pa, $\mu_2 = 0.0086$ Pa, $r_{int} = 44$ μm (from Fig. 3(b)) and $r_{wall} = 100$ μm were used for calculations. E_t was calculated to be 5.27×10^{-5} J m^{-1} s^{-1} in Case 1 (inner (dextran-rich) and outer (PEG-rich) solutions) and 7.47×10^{-5} J m^{-1} s^{-1} in Case 2 (inner (PEG-rich) and outer (dextran-rich) solutions). The viscous dissipation energy of Case 1 was smaller than that of Case 2. The experimental results were shown to correspond with viscous dissipation principles demonstrating the phase configuration of the dextran-rich inner and PEG-rich outer phases.

Conclusions

Phase separation multi-phase flow, especially TRDF, was formed for the first time using a PEG/dextran mixed solution as an aqueous two-phase system. For example, when a mixed solution (PEG 6.4 wt% and dextran 9.7 wt%) was fed into the capillary tube under different conditions, TRDF was observed with inner dextran-rich and outer PEG-rich phases. Proteins, such as BSA, hemoglobin, and lysozyme, were recovered by using a microflow separation system incorporating double capillary tubes, and concentrated in the dextran-rich solution in TRDF. It was found that the present microflow system was useful for separation and extraction of biomolecules such as proteins. The phase configuration of TRDF was also analyzed using viscous dissipation principles.

Acknowledgements

This work was supported by a Grant-in-Aid for Scientific Research (C) from the Ministry of Education, Culture, Sports, Science, and Technology, Japan (MEXT) (No. 17H03083). It was also supported by a grant from Harris Science Research Institute of Doshisha University.

References

1. A. L. Grilo, A.-B. M. Raquel, and A. M. Azevedo, *Sep. Purif. Rev.*, **2016**, *45*, 68.
2. M. Van Berlo, K. C. A. Luyben, and L. A. van der Wielen, *J. Chromatogr. B*, **1998**, *711*, 61.
3. J. A. Asenjo and B. A. Andrews, *J. Chromatogr. A*, **2011**, *1218*, 8826.
4. F. Ruiz-Ruiz F. J. Benavides, O. Aguilar, and M. Rito-Palomares, *J. Chromatogr. A*, **2012**, *1211*, 1.
5. A. Hamta and M. R. Dehghani, *J. Mol. Liq.*, **2017**, *231*, 20.
6. G. Tubio, B. Nerli, and G. Pico, *J. Chromatogr. B*, **2004**, *799*, 293.
7. U. Guenduez and O. M. Dogan, *Chem. Eng. Commun.*, **2005**, *192*, 1586.
8. T. Furuya, Y. Iwai, Y. Tanaka, H. Uchida, S. Yamada, and Y. Arai, *Fluid Phase Equilibr.*, **1995**, *103*, 119.

9. H. Kan, K. Yamada, N. Sanada, K. Nakata, and K. Tsukagoshi, *Anal. Sci.*, **2018**, *34*, 239.
10. K. Nagatani, Y. Shihata, T. Matsushita, and K. Tsukagoshi, *Anal. Sci.*, **2016**, *32*, 1371.
11. K. Kitaguchi, N. Hanamura, M. Murata, M. Hashimoto, and K. Tsukagoshi, *Anal. Sci.*, **2014**, *30*, 687.
12. N. Jinno, M. Murakami, K. Mizohata, M. Hashimoto, and K. Tsukagoshi, *Analyst*, **2011**, *135*, 927.
13. M. Murakami, N. Jinno, M. Hashimoto, and K. Tsukagoshi, *Anal. Sci.*, **2011**, *27*, 793.
14. S. Fujinaga, M. Hashimoto, K. Tsukagoshi, and J. Mizushima, *J. Chem. Eng. Jpn.*, **2015**, *48*, 947.
15. S. Fujinaga, M. Hashimoto, K. Tsukagoshi, and J. Mizushima, *Anal. Sci.*, **2016**, *32*, 455.
16. K. Yamada, H. Kan, and K. Tsukagoshi, *Talanta*, **2018**, *183*, 89.
17. K. Tsukagoshi, *Anal. Sci.*, **2014**, *30*, 65, and references cited therein.
18. K. Tsukagoshi, *J. Flow Injection Anal.*, **2015**, *32*, 89.
19. K. Yamada, N. Jinno, M. Hashimoto, and K. Tsukagoshi, *Anal. Sci.*, **2010**, *26*, 507.